Kinetics of compressive creep in sand cast commercial zinc-based alloys No. 3 and No. 5

A.A. Mir and S. Murphy
Department of Mechanical & Electrical Engineering
Aston University, U.K.

Abstract

Compressive creep tests have been carried out on two sand cast commercial zinc-rich alloys in the stress range 20 to 100 MPa, and at temperatures from 70 to 160°C. A parametric relationship was obeyed, of the form: ln t = C' - n(lnσ) + Q/RT, where C' is a constant, σ the applied stress, t the time of test, n the stress exponent, Q the activation energy, R the gas constant, and T is the absolute temperature.

The primary creep strain increased with copper content and was therefore higher in alloy No5, but the secondary creep rates of No5 were much lower than those of No3. Similarly, time to 1% creep strain was greater for No5. Thus, alloy No5 was found to have a total creep contraction significantly lower than No3 under all testing conditions due to its lower secondary creep rates. The results and structure of alloys showed that creep in alloy No3 is controlled by dislocation climb process, whereas in alloy No5 the creep controlling mechanism is the climb of dislocations over second-phase (ε) particles.

Riassunto

Sono state eseguite su due leghe commerciali ricche di zinco fuse in sabbia delle prove della deformazione permanente da compressione nell'intervallo 20-100 MPa di sollecitazione ed a temperature dai 70 ai 160°C. Il comportamento era consono con un rapporto parametrico del tipo t = C' - n(lnσ) + Q/RT, dove C' è un costante, σ = la sollecitazione applicata, t = il tempo di durata della prova, n = l'esponente della sollecitazione, Q = l'energia di attivazione, R = il costante del gas e T = la temperatura assoluta.

La tensione di deformazione primaria aumenta in funzione del tenore di rame ed è perciò molto più alta nella lega N. 5, mentre la velocità di deformazione secondaria della stessa lega è molto più bassa di quella della lega N. 3. Nello stesso modo, il tempo necessario per il raggiungimento della tensione di deformazione dell'1% è maggiore per la lega N. 5. I risultati hanno dimostrato che nella lega N. 3 la deformazione permanente viene controllata dalla sovrapposizione delle dislocazioni, mentre nella lega N. 5 il meccanismo controllante è la sovrapposizione delle dislocazioni su particelle della seconda fase (ε).

INTRODUCTION

The commercial zinc-based alloys No.3 (Zn-4% Al-0.05% Mg) and No.5 (Zn-4% Al-1% Cu-0.05% Mg) were the first major commercial zinc alloys developed. These alloys are widely used as useful engineering materials especially in automotive industry for many decades. They have a good combination of mechanical and physical properties; particularly relatively low melting temperatures, excellent castability [1] and especially their ability to be cast in the highest speed die-casting machines, long term dimensional stability, fludity characteristics, lower material cost and lower density [2,3,4]. These attributes make them successful competitors against other non-ferrous alloys since their introduction.

It is an important design requirement to determine the compressive and tensile creep of materials used in commercial applications, particularly at moderately elevated temperatures.

Reaserch has been carried out to determine the tensile creep strength of these alloys in the past [5,6,7,8], but so far no attempt has been made to investigate their compressive creep behaviour. Since compressive creep is important in many zinc alloys applications, especially when they are used in automotives where compression is common, it was therefore imperative to study and compare the compressive creep properties of these alloys in detail.

COMPRESSIVE CREEP MACHINE

The machine was designed for compressive creep testing of different materials. Most of the fabrication and machining work of machine has been accomplished in the Manufacturing and Production Engineering Laboratory of Aston University. The machine is of the standard lever loading type with a lever arm ratio of 10:1.

The machine has the following main parts:

1. Three vertical supporting columns with a lever, which is placed on the top of these columns.
2. A hydraulic-jack, which plays an important role in the smooth application of load on the specimen. Initially, the hydraulic-jack sustains the applied load, and then transfers it to the specimen very smoothly at the start of the experiment.
3. An oil-bath, which is used to heat the specimen up to the required constant temperature and maintains it until the termination of the test. The operating temperature of the oil-bath is 45 to 300°C and the extended temperature range with additional cooling is 100 to 300°C. The temperature controller has an accuracy of ± 0.03°C.
4. The strain recording equipment consists of a transducer, strain indicating instrument and the computer. The values of creep deformation are shown according to the time intervals selected in the measurement and control software called 'Windmill'. This software has been purchased so that creep strain can be recorded precisely. The 'Windmill' programme has been modified according to the creep testing requirements. For this purpose, at the start of the test, the time interval between two readings of creep strain is very small, i.e. five seconds, which is increased gradually and eventually the last time interval is one hour. The computer shows the creep data in the form of time (s) versus strain.

EXPERIMENTAL WORK

The specimens used for creep testing were prepared from sand castings of alloys. These specimens were of cylindrical shape, having the following finished dimensions:
length = 30 mm, diameter = 13 mm, bore (plain) = 8 mm.
The alloys used in sand castings were taken from stock materials with guaranteed compositions. The test pieces for all creep experiments were fabricated and machined on a lathe in the Manufacturing and Production Engineering Laboratory of Aston University. During the production of the test samples, the machining operation was carefully controlled so as to reduce variations in surface finish to a minimum.

Compressive creep testing

The specimens were loaded axially in compression and dipped into the oil-bath which was set at the required test temperature. Before the start of the experiment, a reasonably long time was allowed for the temperature of oil-bath and test sample to stablise. The temperature changes of the specimen were kept to a maximum of ±0.5°C for the whole period of the test. The temperature of the specimen inside the oil-bath was measured by a digital potentiometer, using chromel/alumel thermocouples which were attached to the specimen, in order to check for, and thus avoid, any temperature gradients along the gauge length of the specimen.

The resulting creep deformation was recorded in the form of creep strain vs time by the strain recording equipment and displayed by the computer through the "Windmill" measurement and control software, which was designed particularly for these types of tests.

Various stresses from 20 to 100 MPa and temperatures from 70 to 160°C were used during these tests. The experiments were conducted to a minimum creep contraction of 1%.

RESULTS OF CREEP TESTS

Curves of creep strain (%) versus time (ks) were obtained for various combinations of applied stress and testing temperature. Examples of these creep curves have been shown in "figures 1 and 2" for alloys No3 and No5, respectively. From these curves, the primary creep, secondary creep rate and times to achieve total creep strains of 0.5, 0.7 and 1% were also obtained.

Primary creep contraction

Primary creep is defined as the creep deformation obtained by extrapolating the linear secondary creep portion of the creep curve back to zero time. For both alloys, the values of the primary creep (%) were calculated from creep curve of each test. No clear dependence of the primary creep on the testing conditions was observed, but the average values of primary creep for both alloys were generally found to in-

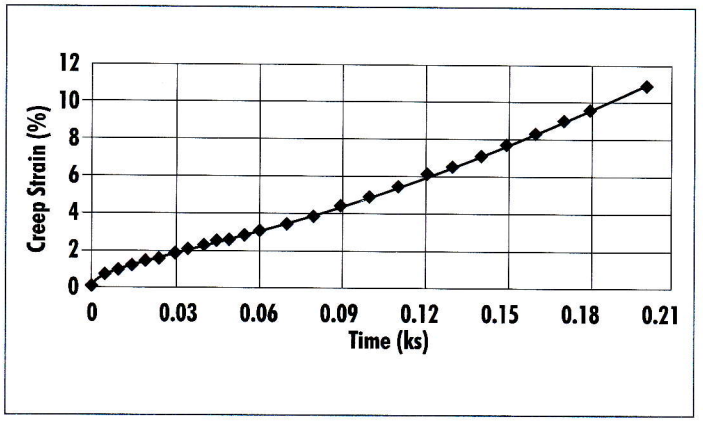

Fig. 1: Creep curve of alloy No3 at 100 MPa and 160°C.

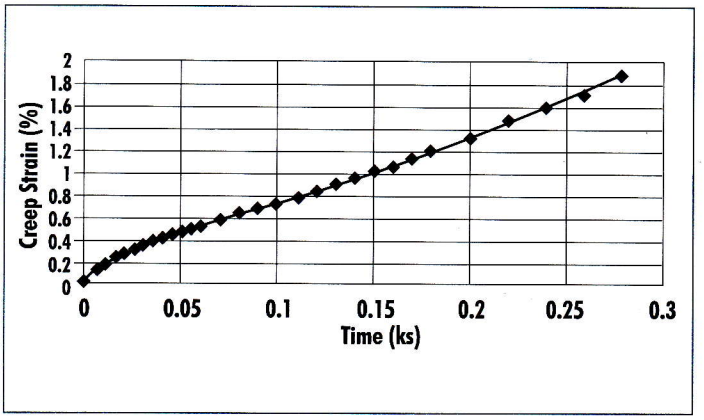

Fig. 2: Creep curve of alloy No5 at 100 MPa and 160°C.

crease with decreasing temperature. The average values of primary creep for each alloy were also found to vary with the copper content. The data showed that it increased with increasing copper content and therefore the average values for alloy No5 were greater than those for No3. The average primary creep contractions versus copper content have been shown in "fig. 3" for both alloys.

Secondary creep rate

Secondary creep rate is the average rate of strain in the linear portion of the creep curve which follows the primary stage. Secondary creep rate has been measured for each test for both alloys and the results plotted in the form of ln secondary creep rate versus ln stress are shown in "figures 4 and 5".

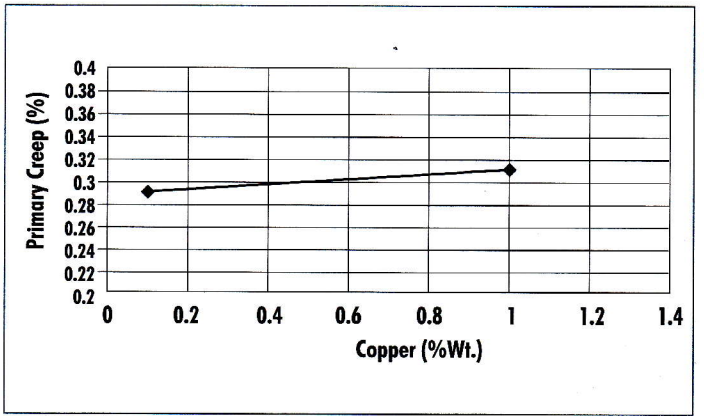

Fig. 3: Variation of primary creep with copper content of alloys No3 and No5.

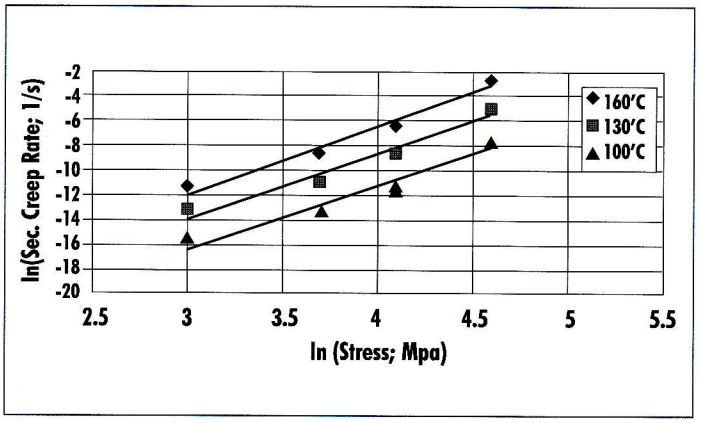

Fig. 4: Variation of secondary creep rates with applied stress at different temperatures for alloy No3

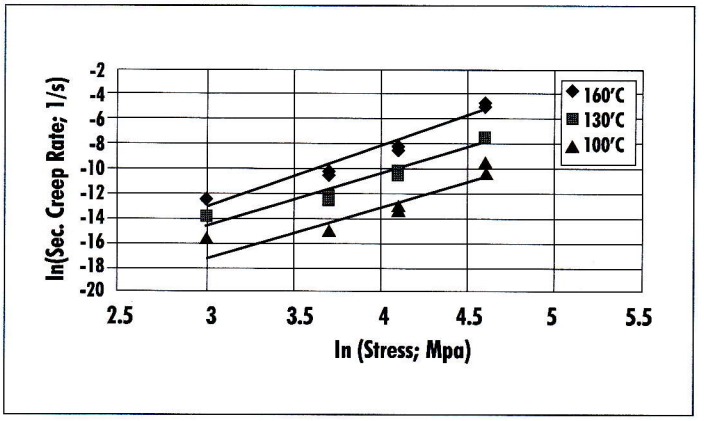

Fig. 5: Variation of secondary creep rates with applied stress at different temperatures for alloy No5

These plots showed a reasonably good correlation with constant slopes for both alloys over much of the stress and temperature range, although deviations were observed at low stresses and low temperatures for both alloys. The average values of slopes (stress exponent) for alloys No3 and No5 were found to be 5.1 and 4.2, respectively. The secondary creep rates (s^{-1}) obtained at 100 MPa are listed in "table 1" for the temperature range of 100 to 160°C for both alloys.

TABLE 1 - Secondary Creep Rates (s^{-1}) of alloys at 100 MPa

Temp. (°C)	100	130	160
No3	4.21×10^{-4}	5.07×10^{-3}	6.04×10^{-2}
No5	4.03×10^{-5}	5.38×10^{-4}	5.30×10^{-3}

Total creep contraction

For both alloys, the times to a total creep contraction of 0.5, 0.7 and 1% were obtained from the creep curves. At different stresses, the log times to 1% creep strain for both alloys were then plotted as a function of the reciprocal of the testing temperature (K), and shown in "figure 6" for 100 MPa. It was observed that these plots were linear with a constant slope (Q/R) over much of the stress range. The average values of the activation energy (Q) for alloys No3 and No5 were calculated as 103 and 108 kJ/mole, respectively. However, deviations from this slope appeared for both alloys at lower stress (40 MPa) and the lowest test temperature of 70°C. The overall creep performances of the alloys as average values of times (ks) to produce 1% creep strain at 100 MPa can be compared from "table 2". This comparison showed that total creep performance of alloy No5 was much better than No3.

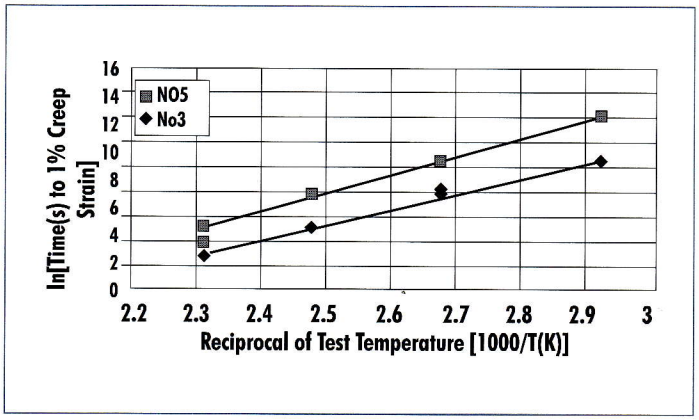

Fig. 6: Ln time to 1% creep strain vs reciprocal of test temperature at 100 MPa

TABLE 2 - Average values of Times (ks) to produce 1% creep strain at 100 MPa

Temp. (°C)	100	130	160
No3	1.425	0.096	0.014
No5	11.890	1.040	0.077

DISCUSSION

From the creep test data of both alloys, it was found that in general alloy No3 had smaller primary creep strain than No5. The mean values of primary creep for alloys No3 and No5 were found to be 0.29 and 0.31%, respectively. These values showed that there was not much difference in the primary creep of alloys. On the other hand, the secondary creep rates of No5 were much lower than those of No3. Since total creep deformation is considered very important design parameter for most creep environments, it is therefore evident that No5 showed a considerably better creep resistance than No3 due to its much lower secondary creep rates. High creep strength of alloy No5 was due to its higher copper content (1%) than No3 which contained only about 0.03 wt. % of copper.

Correlation of creep data

Many researchers [9,10,11] have used the following Arrhenius-type expression to correlate their creep data in metals and alloys:

$$\dot{\varepsilon}_s = A\,\sigma^n \exp(-Q/RT) \qquad (1)$$

This relation was derived from the Norton's power law. Equation (1) may be re-written in the following form:

$$f(\varepsilon) = A\,t\,\sigma^n \exp(-Q/RT) \qquad (2)$$

where A is a constant which takes into account the effects of composition and metallurgical structure, t the creep test time, σ the nominal stress, Q an effective activation energy for creep, R the gas constant, T the absolute test tempera-

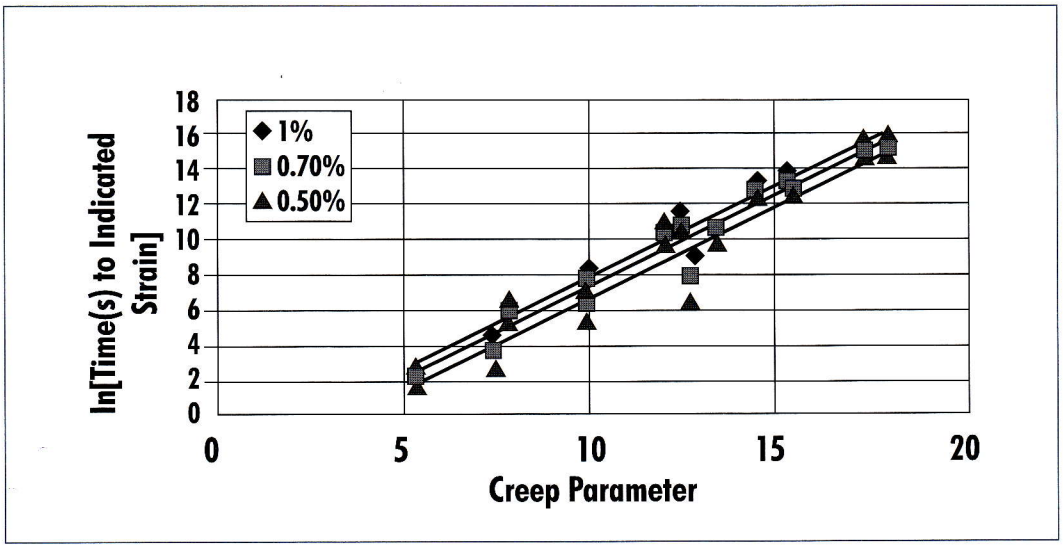

Fig. 7: Ln times(s) to various creep strains vs creep parameter for alloy No3

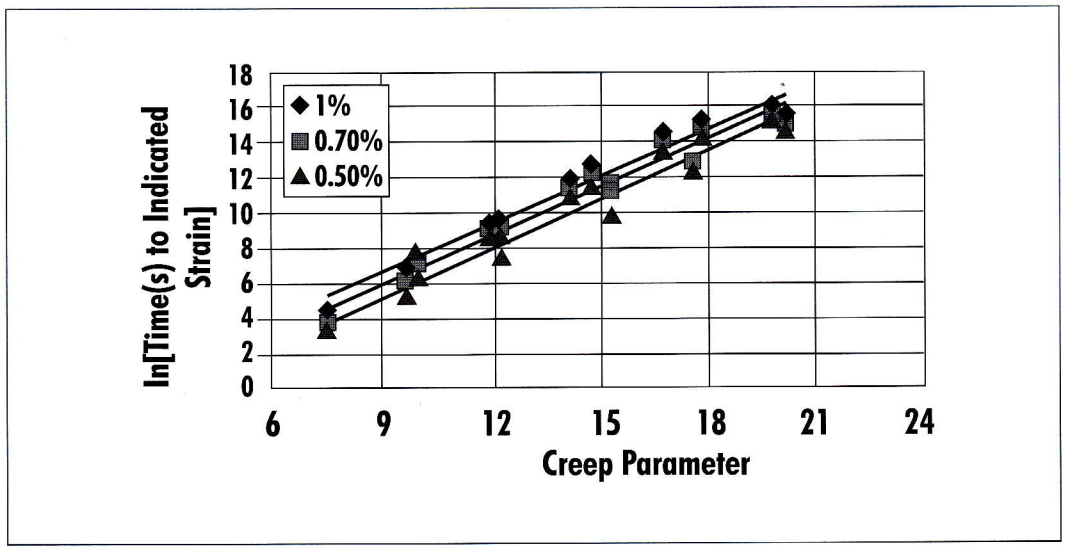

Fig. 8: Ln times(s) to various creep strains vs creep parameter for alloy No5

ture, and f(ε) is an undefined function of the creep strain ε. When A, σ, Q, n and T are constant, f(ε) represents the shape of the creep strain versus time curve. Taking logarithms of equation (2) and rearranging:

$$\ln t = \ln f(\varepsilon) - \ln A - n (\ln \sigma) + Q/RT \qquad (3)$$

and at constant strain:

$$\ln t = C' - n (\ln \sigma) + Q/RT \qquad (4)$$

where C′ is a new constant which incorporates A and ε.

If this relationship is obeyed for the commercial zinc alloys No3 and No5, a plot of ln time to any fixed creep strain against ln stress at a constant temperature should be linear with a slope of -n, or a plot of ln time to any fixed creep strain versus the reciprocal of temperature (1/T) at a constant stress should be linear with a slope of Q/R. Such plots were in fact all linear with constant slopes over the majority of temperatures and stresses used, indicating the stress exponents (n) of 5.1 and 4.2 for alloys No3 and No5, respectively.

The activation energies for alloys No3 and No5 were found to be 103 and 108 kJ/mole, respectively. However, deviations from the constant slope were observed at low stress levels and low temperatures for both alloys.

Thus over a wide range of stress and temperature, the creep behaviour of the alloys has been shown to be related to the testing conditions by an empirical equation, with values of the constants n and Q for both alloys. The ln time to a given % contraction versus the parameter [Q/RT - n (ln σ)] was then plotted, which should give linear plots of unit slope and intercept C′ along the ln time ordinate. C′ is a characteristic constant (creep constant) for the alloy and the chosen creep strain (%). It has been observed [6] that the differences in creep behaviour of the alloys are derived solely from differences in the values of the creep constant (C′).

Using the unsmoothed original data from individual creep curves, graphs of ln time to creep contractions of 0.5, 0.7 and 1.0 % versus the creep parameter for each alloy were drawn, and are shown in "figures 7 and 8". These figures

show that this parameter may be used to estimate the creep behaviour of alloys with high confidence.
The values of the creep constant C' were obtained from the data for both alloys and % contractions, and are given in "table 3". Such data can be used to calculate the design stress which will produce 0.5 %, 0.7 % or 1.0 % creep strain in 100,000 h at different temperatures. The calculated design stresses for alloys No3 and No5 are shown in "table 4".

TABLE 3 - The values of the creep constants C' for alloys No3 and No5

Alloy	Strain (%)	Creep Constant
No3	0.5	-9.04
	0.7	-8.24
	1.0	-7.32
No5	0.5	-5.82
	0.7	-4.85
	1.0	-3.98

TABLE 4 - Maximum continuous design stresses (MPa) for alloys No3 and No5 to produce % strain in 100,000 hours

Temperature (°C)		70	100	130	160
No3	0.5%	6.31	3.14	1.73	1.04
	0.7%	7.62	3.79	2.09	1.25
	1.0%	9.49	4.72	2.60	1.56
No5	0.5%	13.85	6.90	3.80	2.28
	0.7%	17.16	8.54	4.71	2.82
	1.0%	21.02	10.46	5.77	3.46

Microstructural investigations

The as-cast structure of alloy No3 is shown in "fig. 9". The figure showed that the structure of the alloy was heterogeneous and hypoeutectic, consisting of a few large and numerous small primary zinc-rich (η) dendrites. These primary dendritic particles were surrounded by a relatively small volume of lamellar eutectic matrix (α + η). It was also observed that many small rounded dark particles of the Al-rich former β phase were attached to the primary η phase dendrites. These β phase particles were produced during the eutectic solidification. β phase is unstable below about the eutectoid temperature of 275°C and decomposes into Zn-rich η and Al-rich α phases. The edges of the primary η dendrites were also decorated with small and dark Al-rich particles.
The structure of the alloy No3 after being creep-tested in compression at 100 MPa and 160°C, is shown in "fig. 10". The "figures 9 and 10" showed no significant change in the size of primary particles. However, the lamellae of eutectic matrix were well-developed, and were generally smaller than those in the as-cast structure.
The as-cast structure of alloy No5 is shown in "fig. 11". The scale of the structure was similar to that of alloy No3 with more uniformly distributed primary Zn-rich (η) particles. Like alloy No3, the structure of this alloy also consisted of large and small primary Zn-rich dendrites surrounded by lamellar eutectic matrix. The main difference from the structure of alloy No3 was that the size of primary particles in this case was larger as compared to those of No3, also the primary η dendrites and the η component of the (α + η) eutectic had copper-rich ε-phase precipitates, although it was difficult to differentiate these precipitates from zinc (η) particles due to a very small difference in atomic numbers of both zinc and copper. In the structure of alloy No5, the volume of eutectic matrix was relatively small as compared to primary η particles. Many small and dark particles of Al-rich former β phase were observed which were attached to the primary η particles, similar to alloy No3. β is also unstable below about 275°C in alloy No5, and transforms into Zn-rich η and Al-rich α phases.
"fig.12" shows the structure of alloy No5 after compressive creep testing at 20 MPa and 160°C. The volume of eutectic matrix was slightly reduced as compared to the as-cast structure. The micrograph also showed the regular eutectic (α + η) morphology which played an important role in increasing the creep resistance of alloy No5.

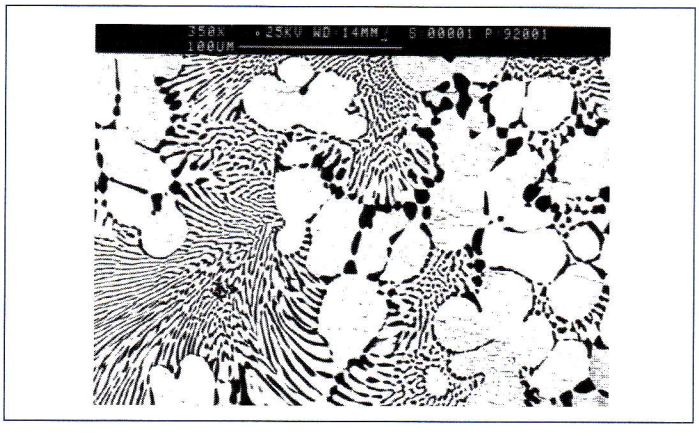

Fig. 9: As-Cast structure (SEM) of Alloy No3, showing primary η dendrites and eutectic (α + η)

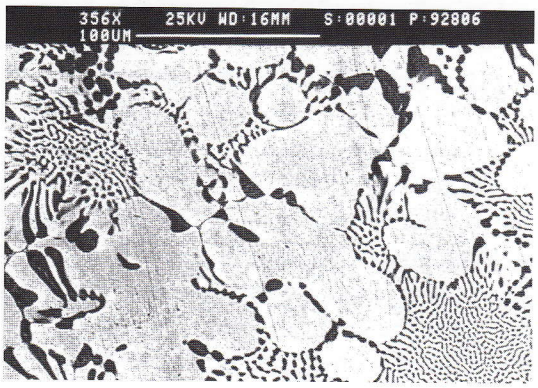

Fig. 10: The structure (SEM) of Alloy No3 tested at 100 MPa and 160°C.

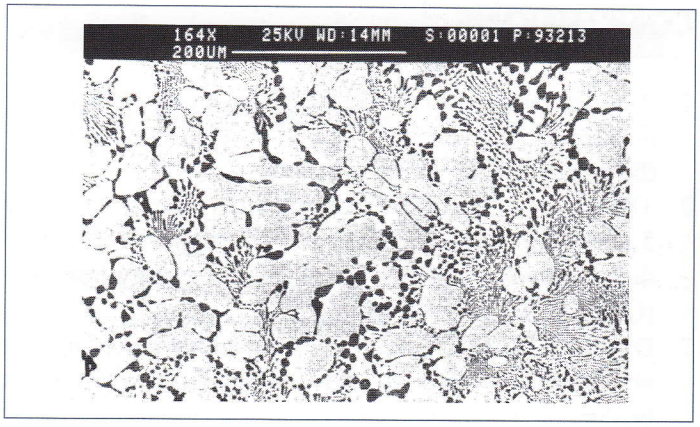

Fig. 12: SEM micrograph of Alloy No5 tested at 20 MPa and 160°C

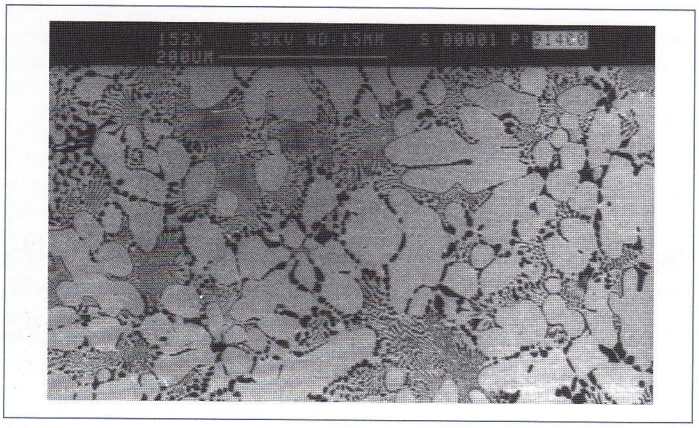

Fig. 11: As-Cast structure (SEM) of Alloy No5, showing large and small primary h particles and lamellar eutectic

Creep mechanisms

A satisfactory procedure of identifying the rate-controlling or dominant creep mechanism may be offered by comparing the calculated values of the stress exponent (n) and the activation energy (Q_c) with the values of these parameters predicted theoretically for different creep processes. Another important consideration for dominent creep mechanism is the analysis of microstructure of the alloys. The values of the stress exponents for alloys No3 and No5 were found to be within the range of 3.0-5.5, indicating Weertman's dislocation climb as the most likely creep mechanism [12]. According to Evans and Wilshire [13], the value of n varies between 4 and 6 for h.c.p. metals. The values of the activation energy for creep for both alloys are very close to those obtained by Durman [14] for Zn-Al alloys No3, ZA.8 and ZA.27. These values also showed that an increase in copper content had increased the value of the activation energy. The values are in excellent agreement with those for self-diffusion in polycrystalline zinc reported by different researchers [15,16], i.e. 91 – 110 kJ/mole.

In many cases, for alloys the activation energy for creep is nearly equal to the activation energy for diffusion of one of the elements, usually the one having the lowest diffusivity and [17] that is zinc in the experimental Zn-Al alloys. The similar values of activation energy for creep (Q_c) and self-diffusion (Q_d) in zinc suggest that the creep rate in the alloys No3 and No5 is diffusion-controlled in the zinc-rich phase for these high temperature creep tests ($T \geq 0.5T_m$).

However, it has been found that the creep resistance of alloy No3 was much lower than alloy No5, and it is believed that the overall better creep strength of alloy No5 was due to the addition of copper content. The lower creep resistance of No3 was mainly due to the lower creep strength of copper-free primary η particles having greater volume than eutectic in the microstructure, as observed in the micrographs. A regular lamellar eutectic ($\alpha + \eta$) morphology combined with the strong strengthening effect of the small particles of ε-phase was primarily responsible for the higher creep resistance of alloy No5 as compared to alloy No3. The similar effects of copper additions on the creep properties of zinc-based alloys have been observed by some other workers [14,18]. The role of these second-phase (ε) particles during creep process is that they act as obstacles to dislocation movement, and therefore reduce the creep rate of alloy No5. Therefore, considering the values of n and Q_c and structural details of alloys, it may be concluded that creep in alloy No3 is controlled by dislocation climb process, whereas in alloy No5 the creep controlling mechanism is the climb of dislocations over second-phase (ε) particles, which was first proposed by Ansell and Weertman [19].

CONCLUSIONS

1. A creep equation of the form: $f(\varepsilon) = A\ t\ \sigma^n \exp(-Q/RT)$ may be used to correlate the total creep contraction of the zinc-rich alloys No3 and No5.
2. The values of the stress exponents (n) were found to be 5.1 and 4.2 for alloys No3 and No5, respectively, while the corresponding values of activation energy for creep (Q) were 103 and 108 kJ/mole.
3. Deviation from the simple creep kinetics occurred in both alloys at low stresses and low temperatures which might be due to changes in the mechanisms of creep.
4. Design stresses calculated from the experimental data revealed that alloy No5 had a substantially better total creep performance than No3 under all testing conditions.
5. The lower overall creep performance of alloy No3 was mainly due to the lower creep strength of primary η particles (copper-free), having greater volume than eutectic in the microstructure. Higher creep resistance of alloy No5 was due to the regular lamellar eutectic morphology combined with the strong strengthening effect of the small particles of ε-phase. These second-phase (ε) particles act as obstacles to dislocation movement, and therefore increase the creep strength of this alloy.
6. In alloy No3, the creep rate is controlled by dislocation climb mechanism, whereas in alloy No5 the creep controlling mechanism is the climb of dislocations over second-phase (ε) particles as proposed by Ansell and Weertman.

ACKNOWLEDGEMENTS

The authors would like to thank Dr. JET Penny Head of the Department of Mechanical and Electrical Engineering at Aston University for providing the laboratory facilities for carrying out the experimental work. Thanks are also due to the staff of the Mechanical and Electrical Engineering Department of Aston University, particularly Messers D. Farmer, Jim Jeffs and P.A. Pizer for their assistance during the tests.

REFERENCES

1. MATHEWSON C.H., in "Zinc-The Science and Technology of the Metal, Its Alloys and Compounds" (Reinhold Publishing Corporation, New York, 1959) p. 21.
2. "Technical Notes on Zinc-Zinc alloy die castings" (Zinc Development Association, London, 1983).
3. "Engineering Properties of Zinc Alloys" (Int. Lead Zinc Research Organization Inc., New York, 1989) pp. 3-8.
4. APELIAN D., M. PALIWAL and D.C. HERRSCHAFT, *J. Met.* 33 (Nov. 1981), 12-20.
5. MURPHY S., T. SAVASKAN and J. HILL, *Can. Metall. Quarterly* 25 (1986), 145-150.
6. MURPHY S., M. DURMAN and J. HILL, *Z. Metallkde.* 79 (1988), 243-247.
7. DURMAN M. and S. MURPHY, *Z. Metallkde.* 82 (1991), 129-134.
8. DURMAN M. and S. MURPHY, in Proceedings of Advances in Science, Technology and Applications of Zn-Al Alloys, Mexico, 1994, edited by G.T. Villasenor, Y.H. Zhu and C. Pina, p. 59-67.
9. R. LAGNEBORG, *Int. Met. Rev.* 17 (1972), 130-146.
10. T. SAVASKAN and S. MURPHY, *Z. Metallkde.* 74 (1983) 78-82.
11. J.D. WHITTENBERGER, E. ARZT and M.J. LUTON, *Scripta Met.* 26 (1992) 1925-1930.
12. J.E. BIRD, A.K. MUKHERJEE and J.E. DORN, in Proceedings of An International Conference on Quantitative Relation between Properties and Microstructure, Jerusalem, 1969, 1969, p. 333.
13. R.W. EVANS and B. WILSHIRE, in "Creep of Metals and Alloys" (The Inst. of Metals, London, 1985) p. 83.
14. M. DURMAN, in "The Creep Behaviour of Pressure Die Cast Zinc-Aluminium Based Alloys" (Ph.D. Thesis, The University of Aston in Birmingham, 1989) p. 204,243.
15. W.J.M. TEGART and O.D. SHERBY, *Phil. Mag.* 5 (1958) 1287-1296.
16. G.A. SIRN, E.S. WAJDA and N.B. HUNTINGTON, *Acta Metall.* 1 (1953) 515-518.
17. F. GAROFALO, in "Fundamentals of Creep and Creep-Rupture in Metals" (The MacMillan Company, New York, 1965).
18. H. NAZIRI and R. PEARCE, *Inst. J. Mech Sci.* 12 (1970) 513-521.
19. G.S. ANSELL and J. WEERTMAN, *Trans. Metall. Soc. AIME* 215 (1959) 838-843.